UCRL- 1597

DECLASSIFIED

SECRET

SECURITY INFORMATION

UNIVERSITY OF CALIFORNIA — BERKELEY

SECRET

SECURITY INFORMATION

RADIATION LABORATORY

DISCLAIMER

UCRL-1597
Special Distribution

SECRET
SECURITY INFORMATION

UNIVERSITY OF CALIFORNIA

Radiation Laboratory

Contract No. W-7405-eng-48

CLASSIFICATION CANCELLED
BY AUTHORITY OF THE DECLASSIFICATION BRANCH USAEC
BY B. Foskett 2-28-56
SIGNATURE OF THE PERSON MAKING THE CHANGE DATE

PRELIMINARY CONSIDERATIONS REGARDING STABILITY OF MTA MARK I AS A CLOSED-LOOP SYSTEM

J. F. Waddell

November 1, 1951

RESTRICTED DATA

This document contains restricted data as defined in the Atomic Energy Act of 1946. Its transmittal or disclosure of its contents in any manner to an unauthorized person is prohibited.

Berkeley, California

SECRET
SECURITY INFORMATION

SUBJECT: Preliminary Considerations regarding Stability of MTA Mark I as a Closed-loop System

NAME: J. F. Waddell

DATE: 1 November 1951

The basic scheme under consideration in this research on stability of closed-loop operation of the Mark I machine is one in which a voltage proportional to the magnitude of the rf fields in the cavity acts to control rectifier voltage output. It is recognized that such is not the only scheme for maximization of output which may be conceived, but only what seems to be a logical and direct way of attaining such an objective.

The program under discussion consists of experimental and theoretical attempts to devise a model, which for purposes of this work, will disclose the dynamic behavior of the Mark I MTA. It would seem that the most direct approach would be to seek a model having the form of an electrical network, and this approach has been used. Thus, since in the sense of this problem the Mark I machine is a two-terminal-pair network, the substitution of a model of the same generic class makes possible the production on a laboratory scale of the anticipated characteristics of the large machine.

It has for many years been customary, in dealing with feedback systems, to use as a guide the stability criterion of Nyquist[1], wherein stability is judged by the behavior of the open-loop transfer function of the system on the complex plane. This criterion defines the term "stable" to mean that condition wherein the transient response of the system to an input signal perturbation will eventually decay to z ero, i.e., the transient term will have a negative, rather than a positive exponent. Such a criterion does not yield sufficient information, for although it recognizes "black" as being black, it groups "white" and "gray" into a class of things "not black". Indeed, under the conditions outlined in the first paragraph, it is found that while the Mark I machine can be, with a fair degree of confidence, expected to be "not black", it seems fairly certain to be "not white". To be explicit, the work to date indicates strongly that there are to be expected overshoot and damped oscillatory responses to perturbations in operating variables arising anywhere within the system.

The above remarks should not be interpreted in a pessimistic sense, i.e., the writer is not predicting the disintegration of Mark I the moment it is turned on! Difficulties of the nature of those likely to be encountered are well subject to reduction by means of electrical networks (phase-correction networks) appropriately located in the loop, thereby making available the refinement of control obtainable in an r-f stabilized system, while maintaining adequate stability.

Performance of the system under closed-loop conditions must be calculated by means of the relation[2]

$$\bar{v}(\omega) = \frac{v(\omega)}{1 + v(\omega)} \qquad (1)$$

where $\bar{v}(\omega)$ is the transfer function (ratio of output voltage to input voltage) for the system under closed-loop conditions, and $v(\omega)$ is the open-

(1) Nyquist, Bell System Technical Journal, 11, 126 (1932)

(2) "Electronic Instruments", M.I.T. Rad. Lab. Series, Vol. 21 (McGraw, 1948) Chapters 9 to 11, (in particular Sec. 9.4)

loop transfer function.

This calculation may be performed graphically by superposing on the plane of the open-loop transfer function (the v-plane) a set of bipolar coordinates which are appropriately normalized (see fig. 6). Such a plot has the considerable advantage of not only showing that something is wrong (assuming for the moment that something is wrong) but evaluates both the trouble, and projected remedial measures quantitatively.

Having mentioned briefly the method of predicting closed-loop performance, one turns now to discussion of open-loop performance, from which, as has been noted, closed-loop performance is directly predictable. In the system under discussion the rectifier equivalent circuit has been temporarily assumed to be a black box with unity transfer function - i.e., the internal impedances of energy source and rectifier have been neglected. This has been done because a firm decision regarding the exact nature of the rectifier and energy source has not been reached -- the data on this subject has only recently become available.

Our experiments indicate to a considerable degree of certainty that a small signal equivalent circuit for the oscillators and cavity, valid in a time-domain whose units are such that a period of oscillation at the cavity resonant-frequency (approximately 10^{-7} sec.) is negligibly small compared therewith, is the resistance-capacitance combination shown in figure 1.

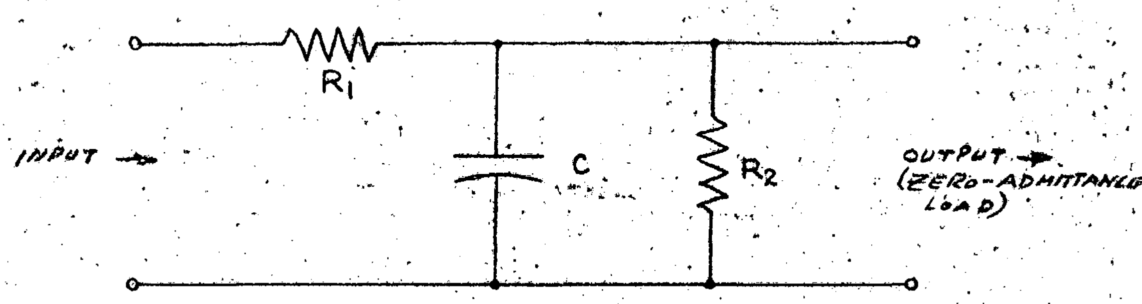

Figure 1 Small-signal equivalent circuit used for oscillator and cavity in time-domain defined in text.

R_1 accounts for oscillator losses, and R_2 for cavity losses. R_2C is just the time constant of the cavity under whatever loading conditions are being considered (i.e. beam-on or beam-off). Discussion of the reasons behind such a conclusion are somewhat lengthy, and will be dealt with in a more complete report to follow.

The complete network, to which the curves apply, is shown in figure 2, which is identical with figure 1 except for the addition of a series inductance element, L, which is the smoothing reactor. Derivation of the transfer-function of this network, and an outline of the calculations of the parameters thereof, from which the curves were calculated, are to be found in the appendix.

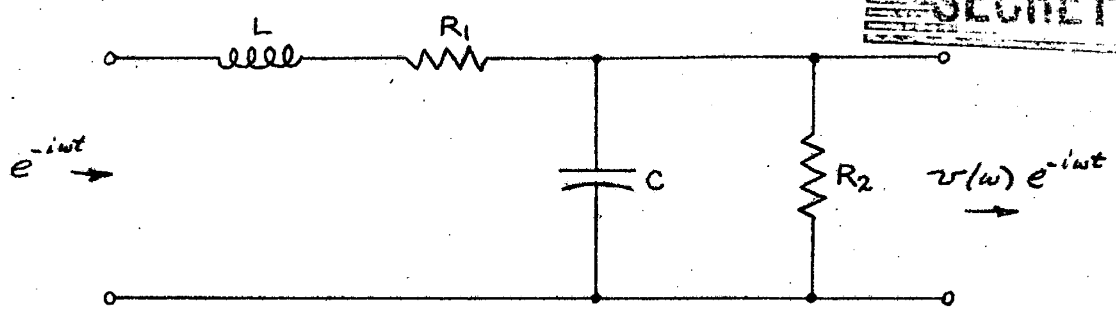

Figure 2 Small-signal equivalent circuit used for calculation of open- and closed-loop performance data (preliminary).

In examination of the curves it will be noticed that three values of L are used, 8, 12, and 20 millihenries, representing inductance values for the three possible modes of connection for the inductor in question. Beam-off and beam-on conditions are distinguished by grouping the curves: curves number 1, 2, and 3 are for beam-on condition; curves 4, 5, and 6 are for beam-off. Curves 1 and 4, 2 and 5, 3 and 6, are for 8, 12, and 20 millihenries respectively, as noted in the figure.

Explanation of the curves follows

Figures 3, 4 and 5 show the transfer functions for the equivalent circuit of figure 2. under the conditions previously outlined. It should be noted that normalization is such that the curves as shown apply to unity gain with beam-on, 1.05 gain with beam-off. The number 1.05 is the approximate predicted change in output voltage for the actual system when the beam is turned off. To consider the system with any value of gain $g \neq 1$, the critical point on the Nyquist diagram (i.e., the point $-1 + i0$) is here transformed into the point $-\frac{1}{g} + i0$.

It is to be noted that since for all cases the phase-shift asymptote is $-\pi$ the loci cannot encircle the critical point. For gains equal to or greater than five the phase margins are always less than approximately 30 degrees. With this observation we discard the essentially qualitative concept of phase margin and deal with the closed-loop transfer function, which gives a quantitative account of system behavior under closed-loop conditions.

Figures 6 and 7 show the superposed equal-amplitude and equal-phase contours for the function $\frac{v}{1+v}$ superposed upon the open-loop transfer function (v), i.e., the $\bar{v}$-plane is transformed into the v-plane (see eq. 1). Only the critical region is shown, and, of course, the function v is no longer normalized. Shown are loci of v for two values of gain, 5 and 10, between which, it is estimated, the necessary value of system loop gain will lie. $|\bar{v}|$ and $\mathrm{Arg}(\bar{v})$ may be tabulated from intersections of these contours with the loci of v. These functions are displayed in figures 8 to 15.

Figures 8, 9, 10, and 11 compare $\bar{\bar{v}}(\omega)$ for gains of 5 and 10 with $\bar{v}(\omega)$. It is readily seen that whatever trouble arises in the closed-loop system, it is in that region of the frequency domain occupied by the critical region of the v-plane, or Nyquist diagram, a frequency region where v is "down in the mud" if loop gain is even moderate. The phase-function, Arg($\bar{v}$) is confined to small values until the critical region of v is reached, whereupon rapid increase of phase-shift with frequency occurs. The frequency of peak amplitude and of $\frac{\pi}{2}$ phase-shift are close, the more so at higher gains. The whole thing adds up to a quasi-resonant type of behavior in which the "stable" system, i.e., the system in which oscillations will not build up, is yet an underdamped system which when pulsed will "ring". Decrement of the oscillations is determined by damping of the system itself (see Fig. 12 to 15) as well as by the loop gain. From the relation $Q = \frac{\Omega}{\delta\Omega}$ where Ω is the resonance frequency and $\delta\Omega$ is the frequency interval between the points for which $|\bar{\bar{v}}| = \frac{|\bar{v}(\omega)|}{\sqrt{2}}$ we find that for beam-on, $Q_{10} \cong 3.75$, $Q_5 \cong 2.25$ and for beam-off $Q'_{10} \cong 3.80$, $Q'_5 \cong 2.93$. Since critical damping occurs for $Q = 1/2$, the system is clearly underdamped for all conditions. Experiments performed on a model show the existence of damped oscillations in response to any small perturbation of the system.

As has been mentioned previously, this situation is subject to correction. One remedy first suggesting itself is a "phase-lead" network having time-constants so adjusted as to warp the critical region of the v-locus in the direction of decreased $\bar{\bar{v}}$. The situation will be dealt with at length in the report to follow.

It is hoped that these notes will show that there may be a problem, together with a semi-quantitative notion as to its magnitude. Work on the equivalent-circuit problem is continuing apace, preparations are being made to collect data on a laboratory-scale oscillator using the 12 mc/sec reentrant cavity made up for the Q-measurement group. Remaining yet is a series of data to be taken in the frequency domain (sinusoidal modulation of plate voltage) to be performed on both the lumped-circuit and cavity apparatus. To date all data has been taken in the time domain (pulse modulation).

Present plans for start up of Mark I include only stabilization of oscillator (dc) plate voltage. The scheme herein discussed is one suggested by Panofsky primarily for application to Mark II. It goes without saying that the logical way in which to start such an investigation with regard to Mark II is to investigate the properties of Mark I in this respect and if possible make an experimental check on the machine itself.

It should be here pointed out that little difficulty should be encountered in conversion, on either a temporary or permanent basis, of the initial system for regulation of oscillator (dc) plate voltage to the scheme under consideration. Any rf level monitoring signal from the cavity may be used, with the requisite loop gain provided by the vertical amplifier from any dc oscilloscope, which would have more than sufficient output necessary to drive the existing equipment.

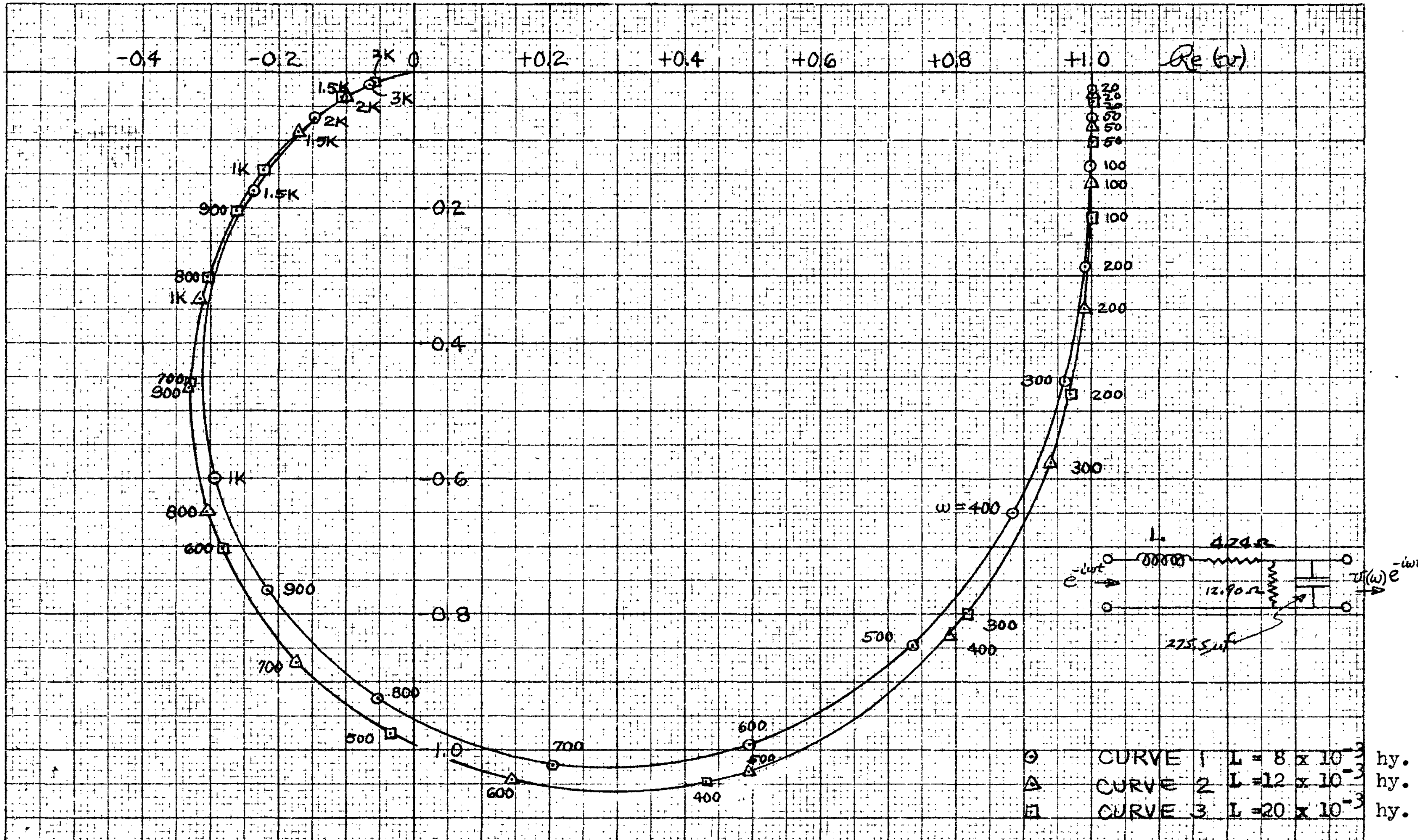

Figure 3
NORMALIZED OPEN-LOOP TRANSFER FUNCTION
(Nyquist Diagram)
Beamron Condition, source impedance of rectifie r neglected.

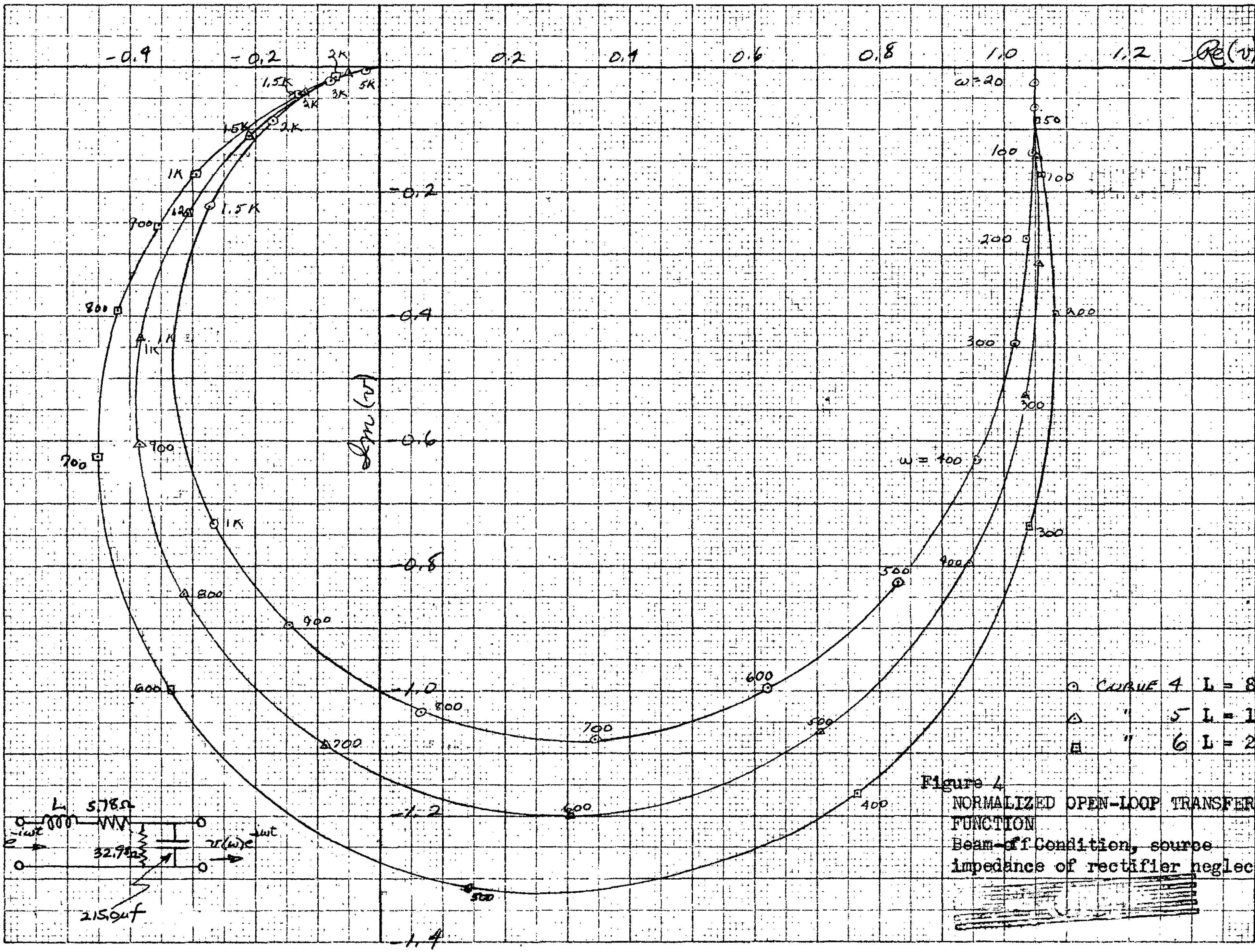

Figure 4
NORMALIZED OPEN-LOOP TRANSFER FUNCTION
Beam-off Condition, source impedance of rectifier neglected

186441

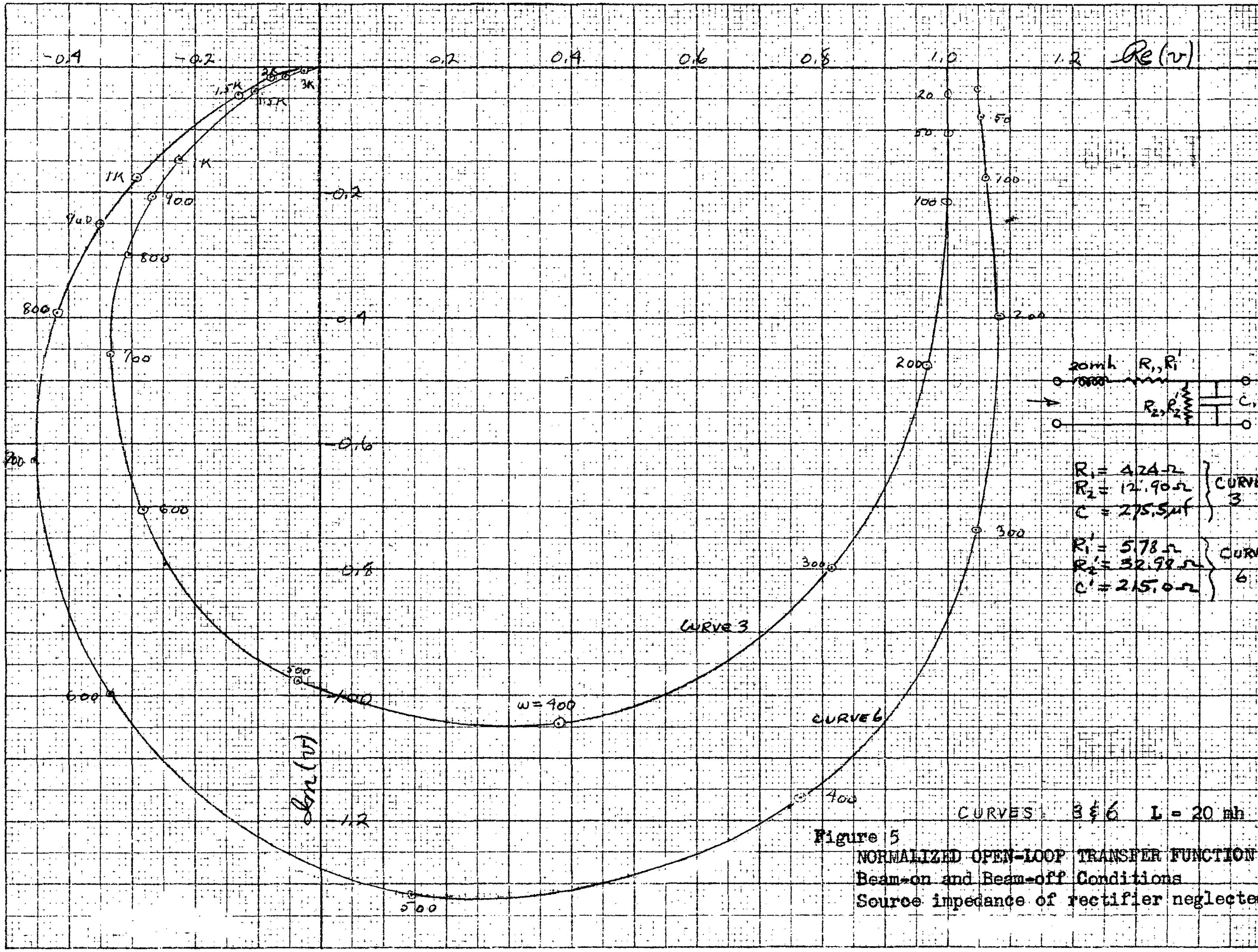

Figure 5
NORMALIZED OPEN-LOOP TRANSFER FUNCTION
Beam-on and Beam-off Conditions
Source impedance of rectifier neglected.

186451

SECRET

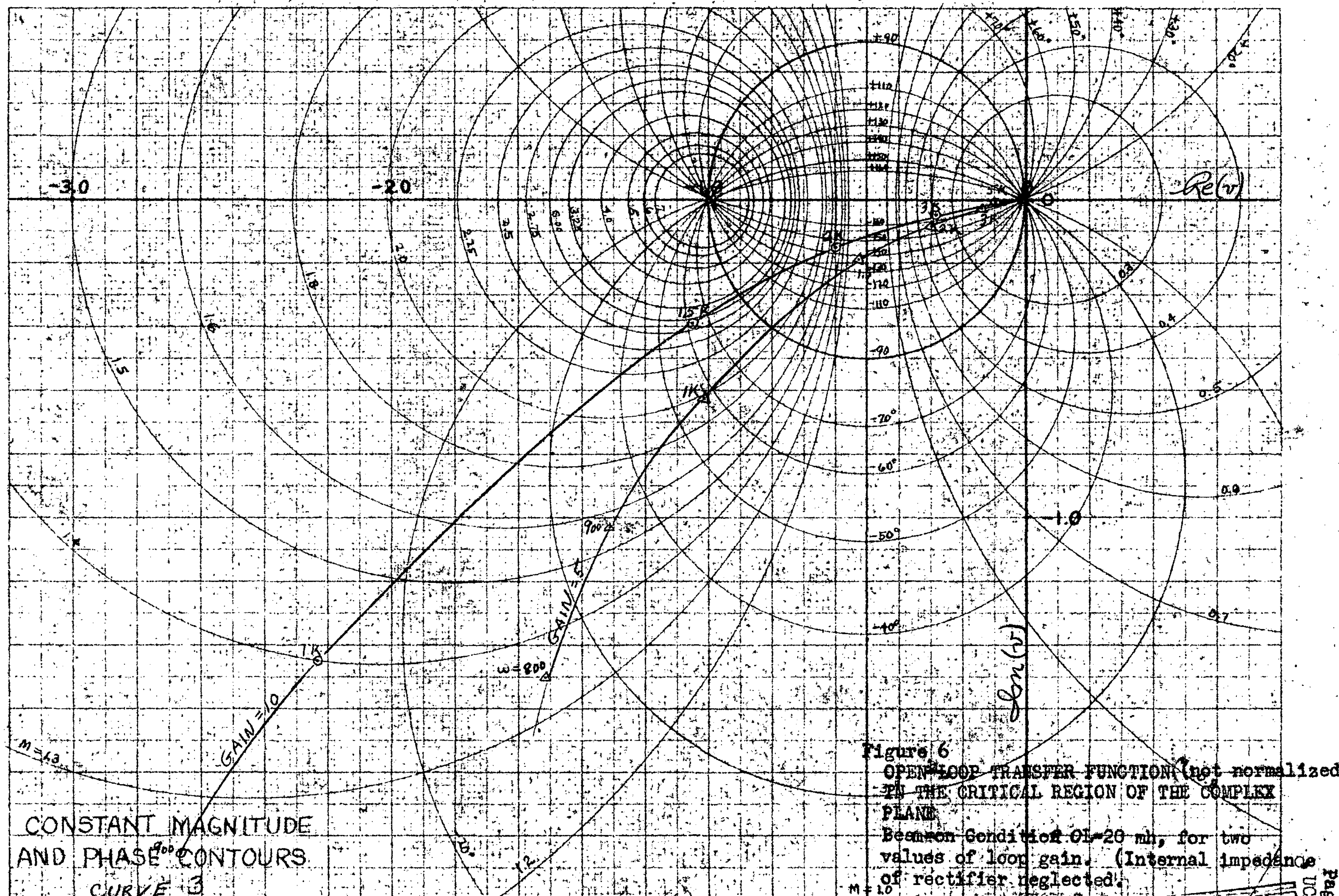

Figure 6
OPEN-LOOP TRANSFER FUNCTION (not normalized) IN THE CRITICAL REGION OF THE COMPLEX PLANE
Beamon Condition OL=20 mh, for two values of loop gain. (Internal impedance of rectifier neglected).

SECRET

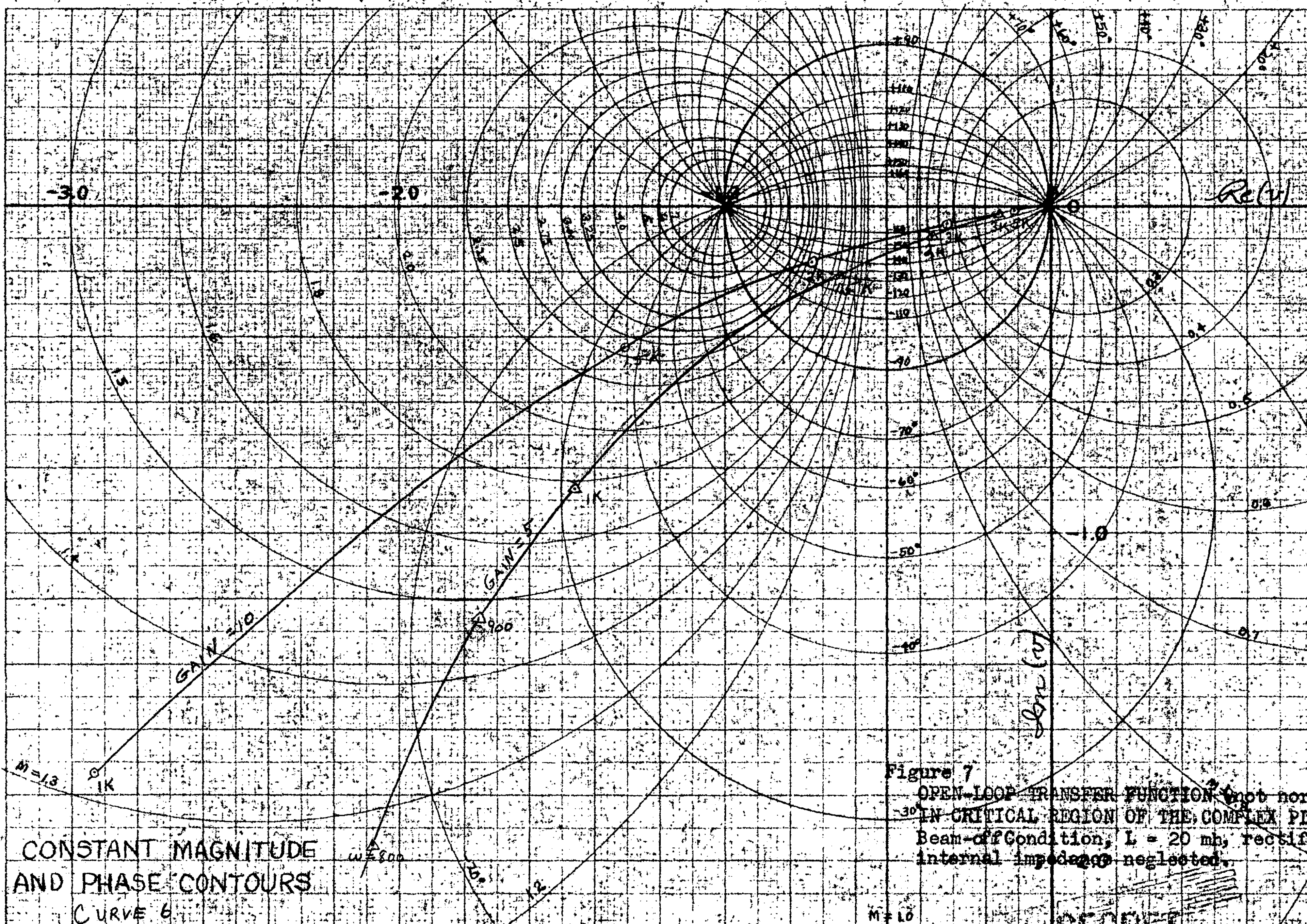

Figure 7
OPEN-LOOP TRANSFER FUNCTION (not normalized
IN CRITICAL REGION OF THE COMPLEX PLANE
Beam-off Condition, L = 20 mh, rectifier
internal impedance neglected.

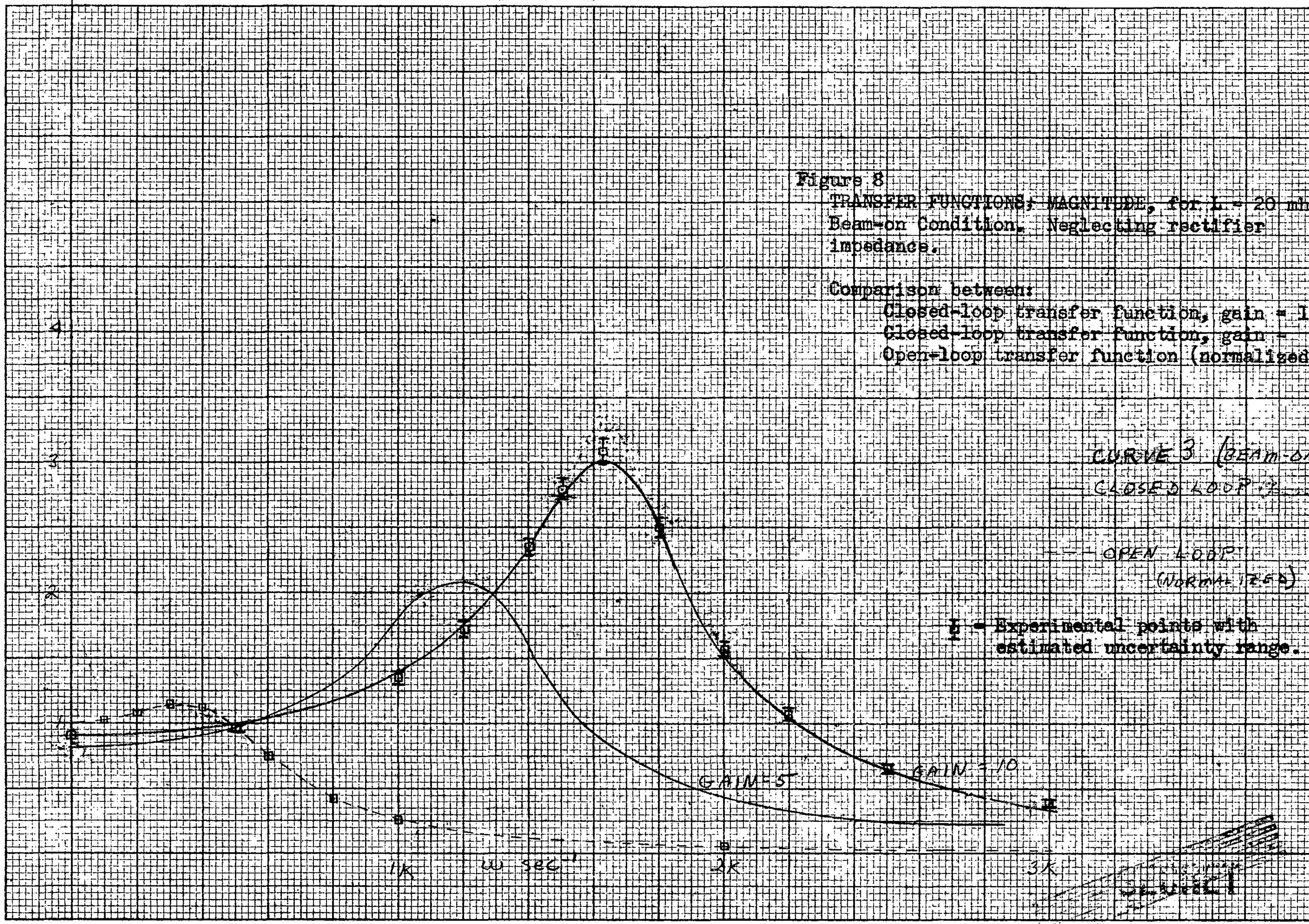

Figure 8
TRANSFER FUNCTIONS, MAGNITUDE, for L = 20 mh
Beam-on Condition. Neglecting rectifier impedance.

Comparison between:
Closed-loop transfer function, gain = 10
Closed-loop transfer function, gain = 5
Open-loop transfer function (normalized)

Ĭ = Experimental points with estimated uncertainty range.

186481

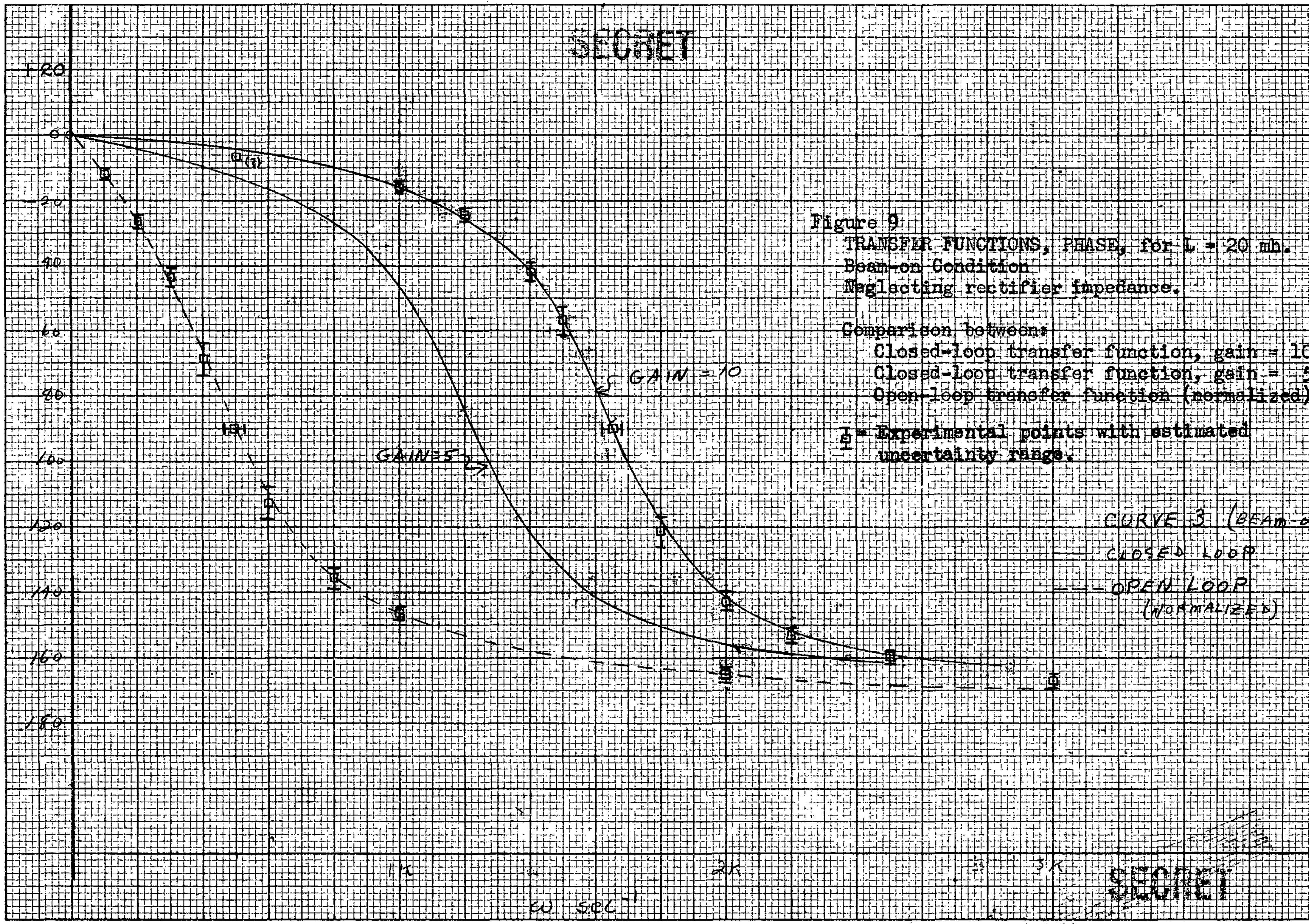

Figure 9
TRANSFER FUNCTIONS, PHASE, for L = 20 mh.
Beam-on Condition
Neglecting rectifier impedance.

Comparison between:
Closed-loop transfer function, gain = 10
Closed-loop transfer function, gain = 5
Open-loop transfer function (normalized)

⌶ = Experimental points with estimated uncertainty range.

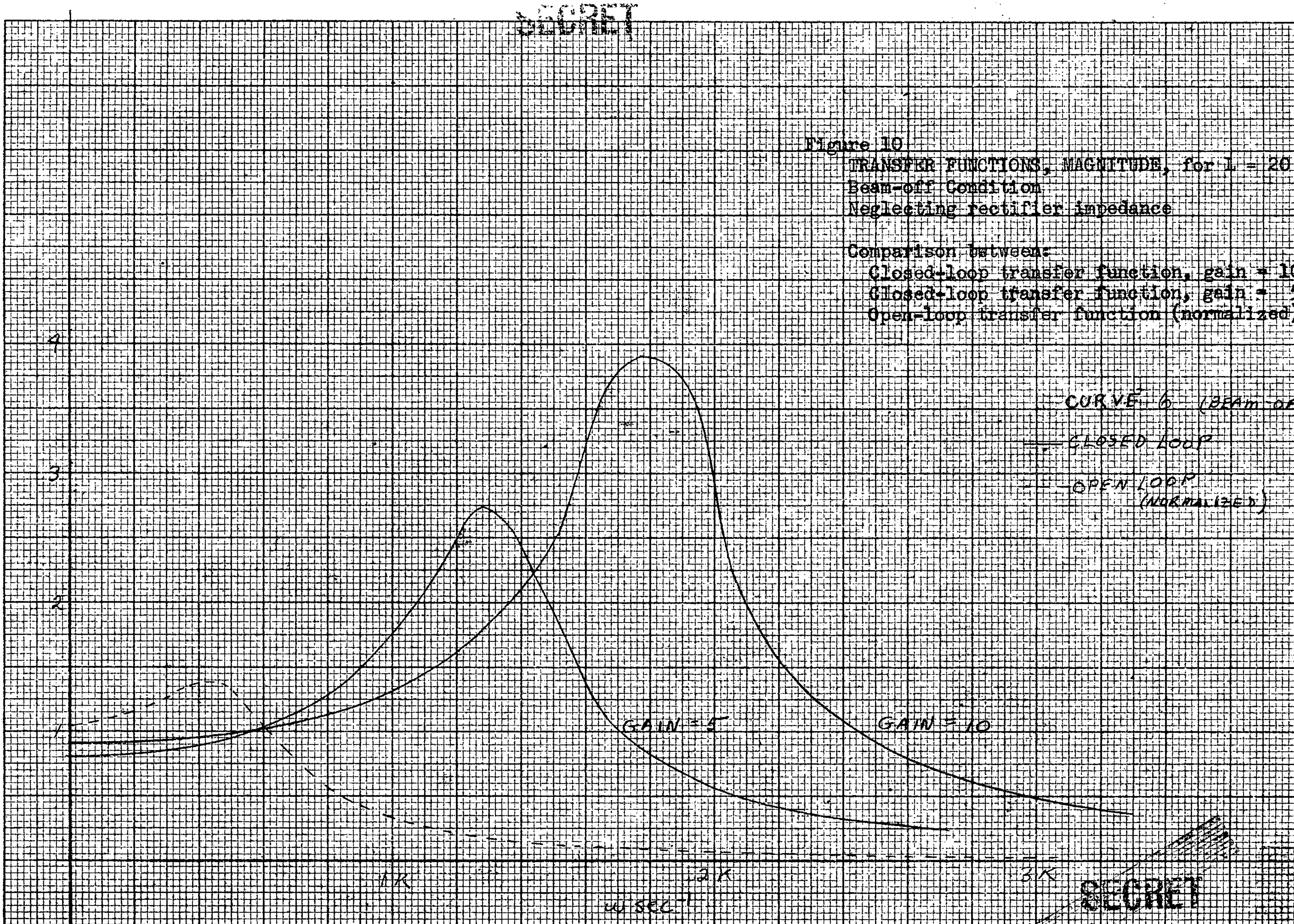

Figure 10
TRANSFER FUNCTIONS, MAGNITUDE, for L = 20 mh
Beam-off Condition
Neglecting rectifier impedance

Comparison between:
Closed-loop transfer function, gain = 10
Closed-loop transfer function, gain = 5
Open-loop transfer function (normalized)

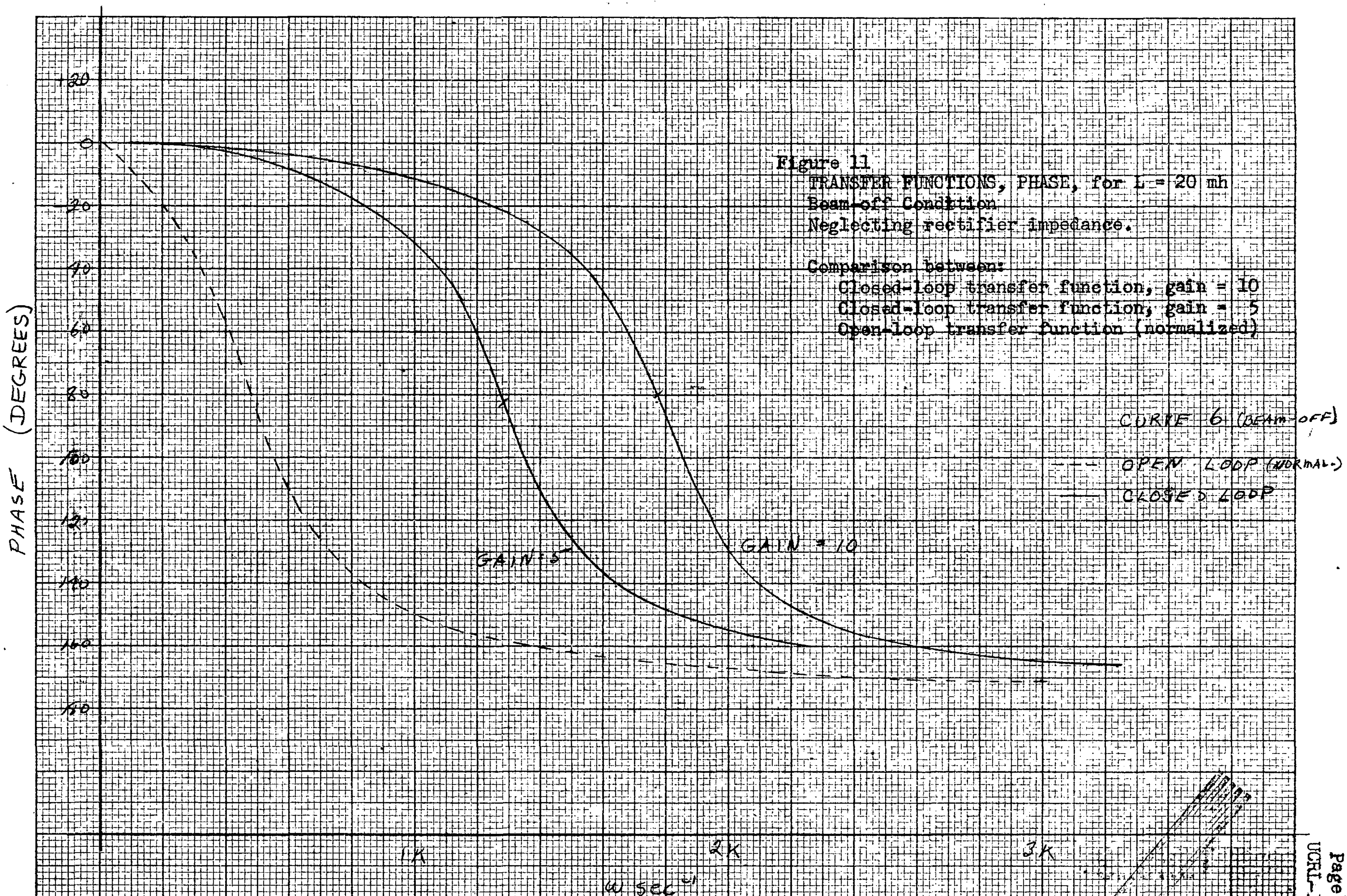

Figure 11
TRANSFER FUNCTIONS, PHASE, for L = 20 mh
Beam-off Condition
Neglecting rectifier impedance.

Comparison between:
Closed-loop transfer function, gain = 10
Closed-loop transfer function, gain = 5
Open-loop transfer function (normalized)

186511

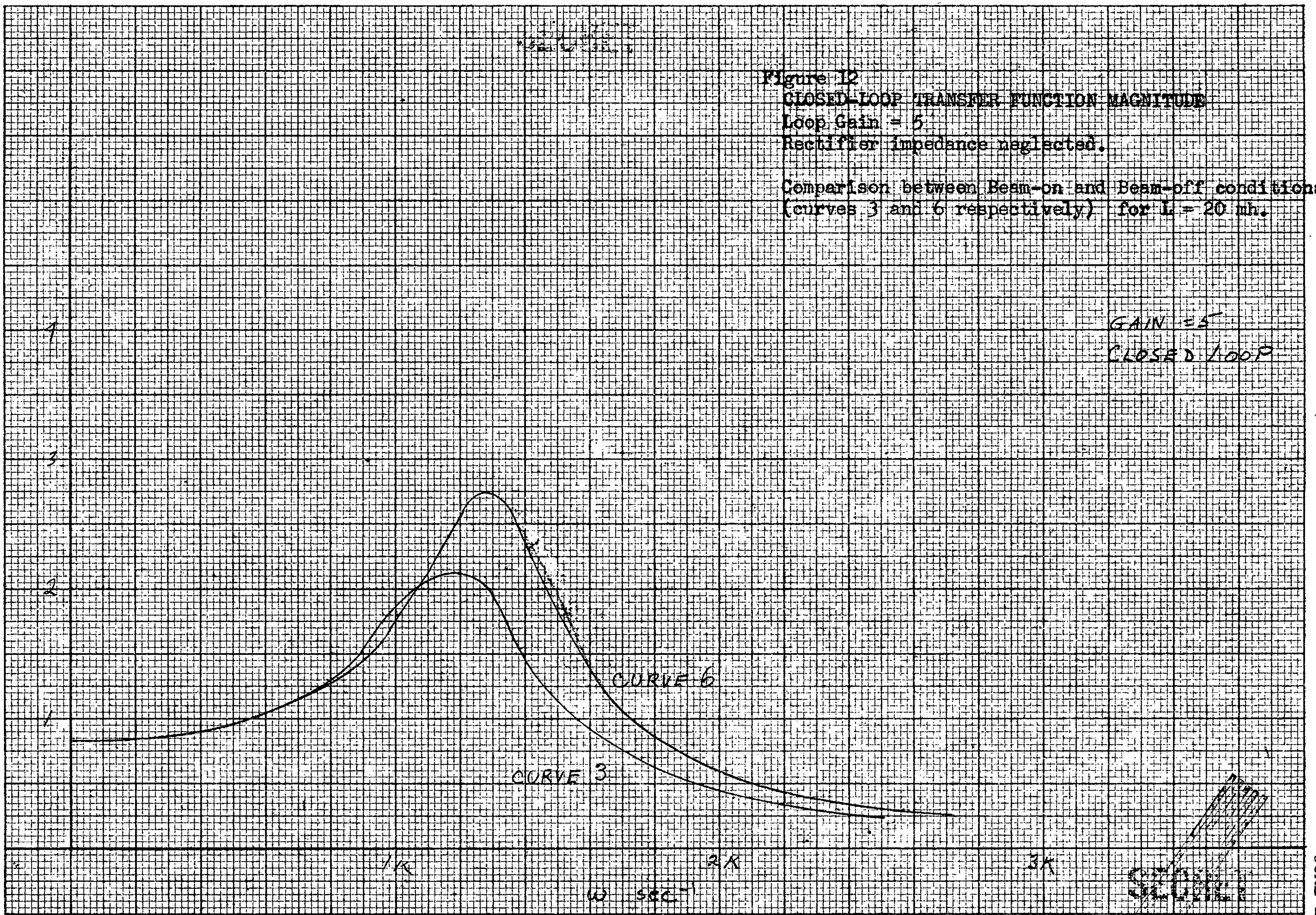

Figure 12
CLOSED-LOOP TRANSFER FUNCTION MAGNITUDE
Loop Gain = 5
Rectifier impedance neglected.

Comparison between Beam-on and Beam-off conditions (curves 3 and 6 respectively) for L = 20 mh.

186521

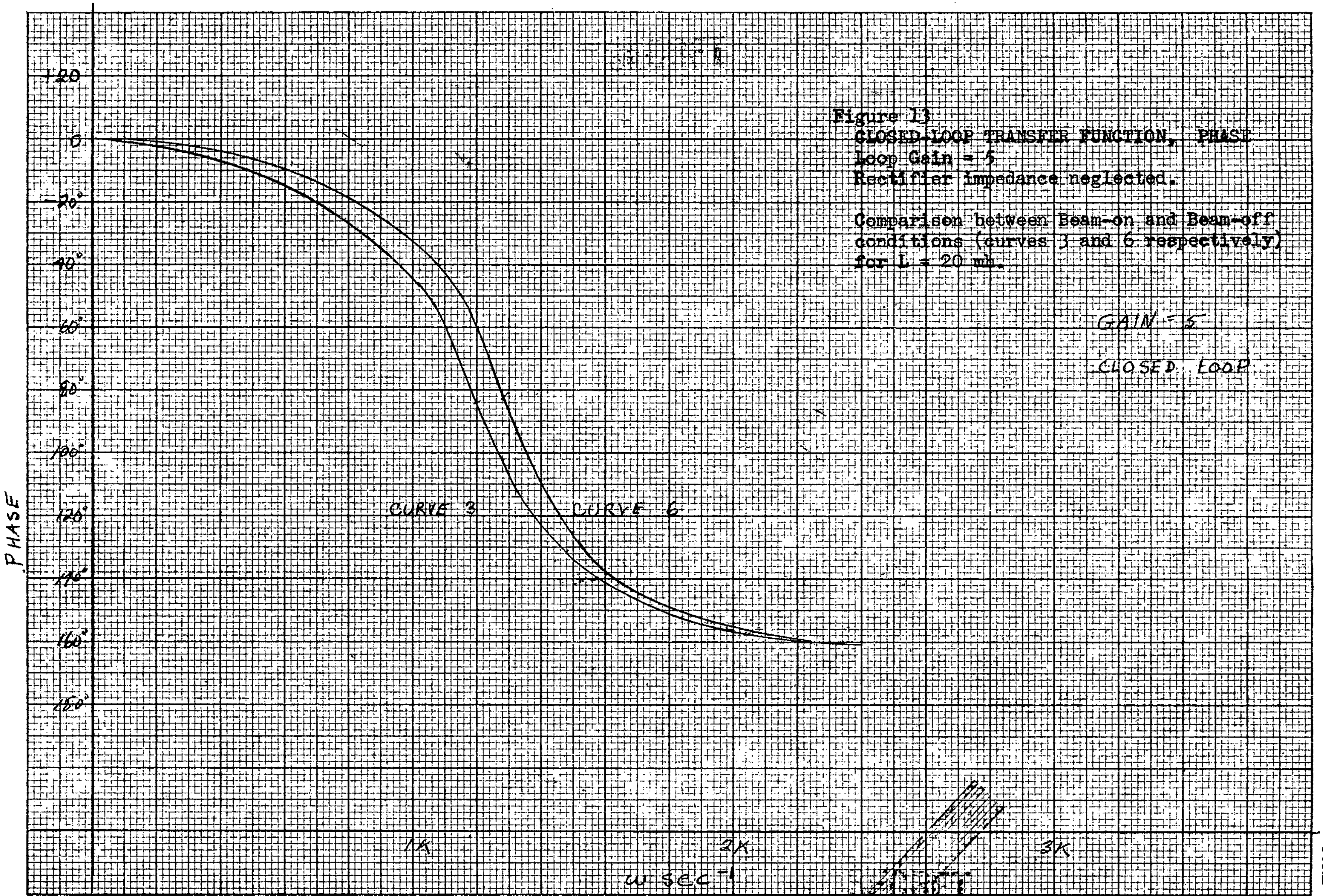

Figure 13
CLOSED-LOOP TRANSFER FUNCTION, PHASE
Loop Gain = 5
Rectifier impedance neglected.

Comparison between Beam-on and Beam-off conditions (curves 3 and 6 respectively) for L = 20 mh.

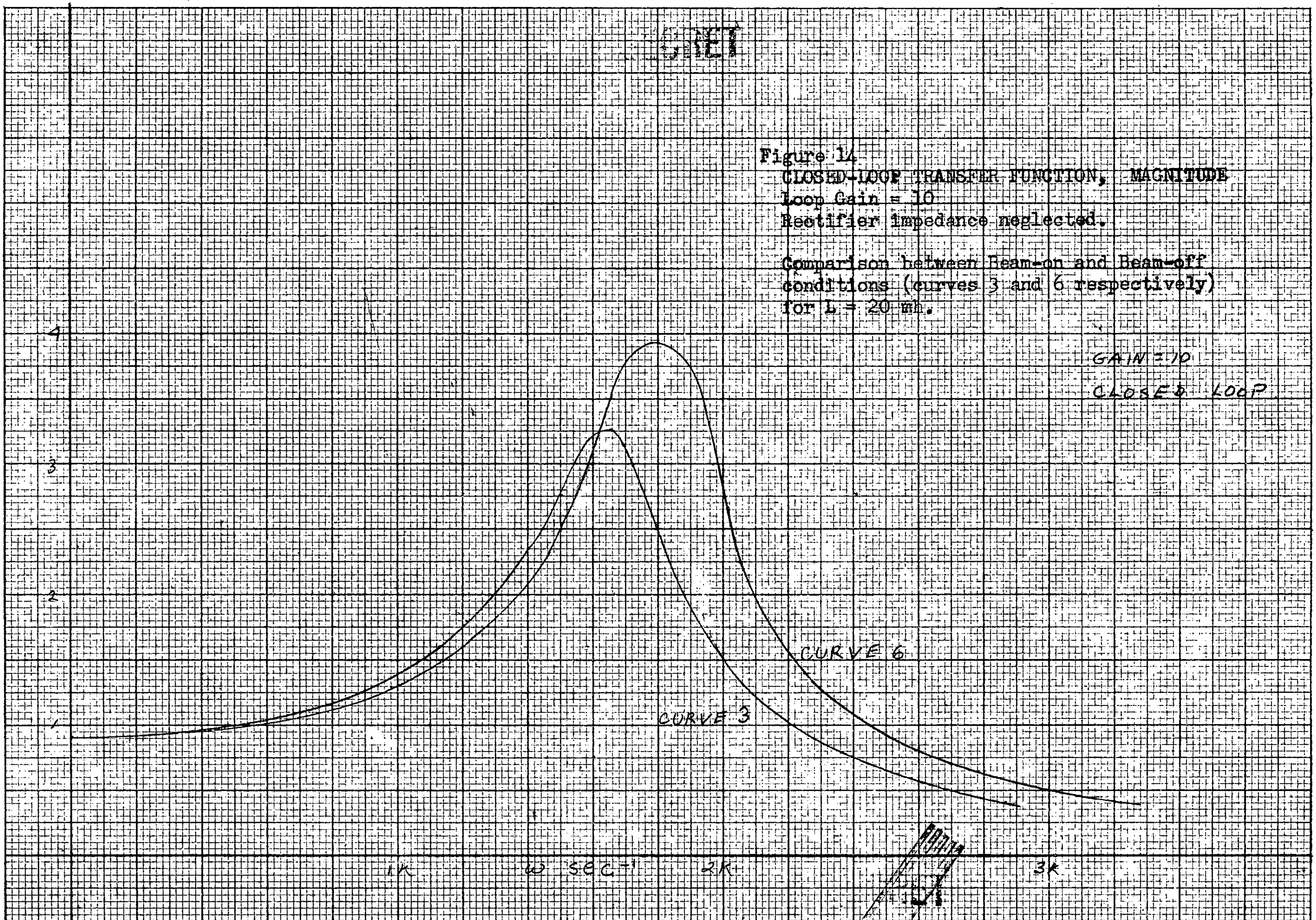

Figure 14
CLOSED-LOOP TRANSFER FUNCTION, MAGNITUDE
Loop Gain = 10
Rectifier impedance neglected.

Comparison between Beam-on and Beam-off conditions (curves 3 and 6 respectively) for L = 20 mh.

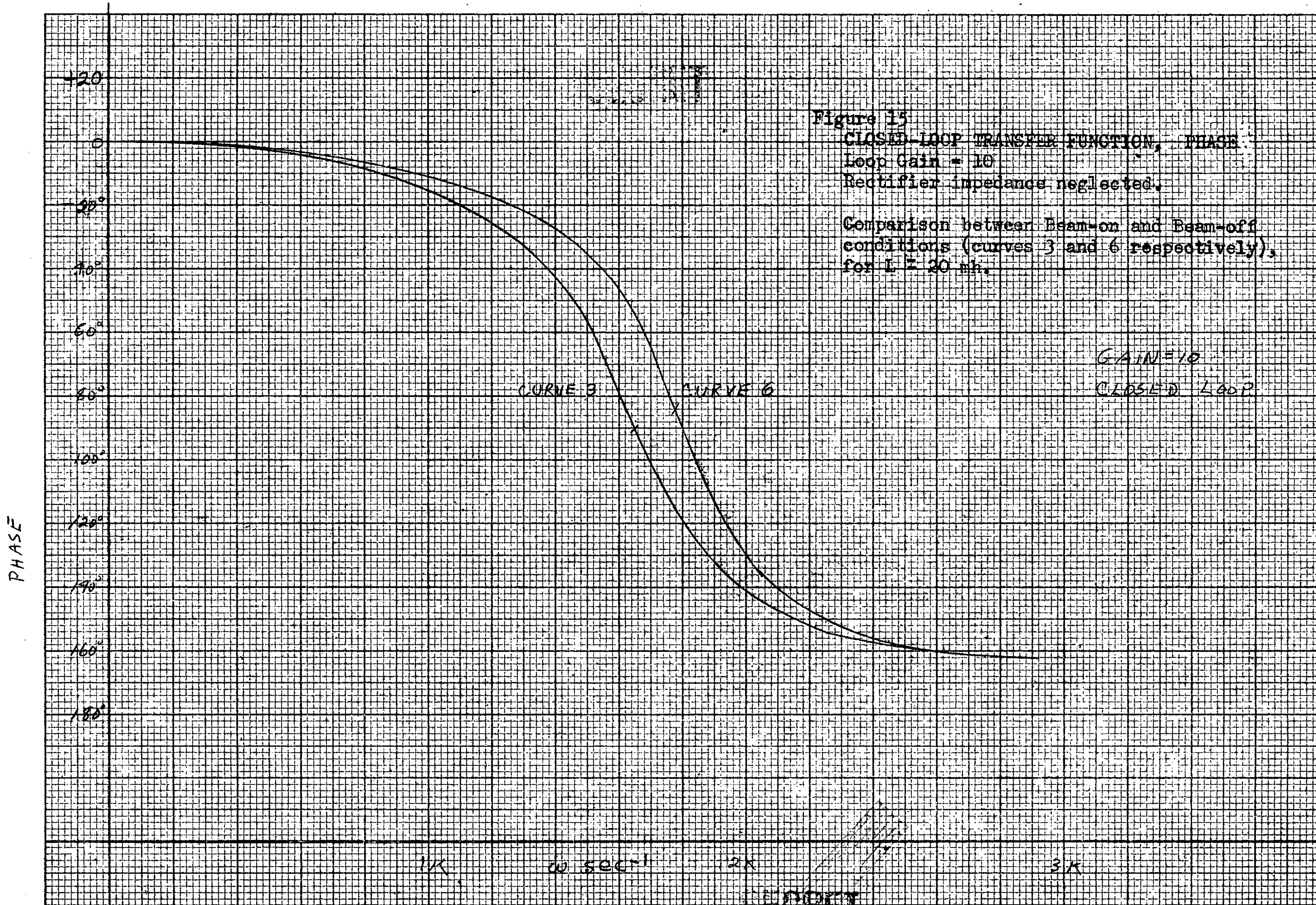

Figure 15
CLOSED-LOOP TRANSFER FUNCTION, PHASE
Loop Gain = 10
Rectifier impedance neglected.

Comparison between Beam-on and Beam-off conditions (curves 3 and 6 respectively), for L = 20 mh.

SECRET

186551

SECRET

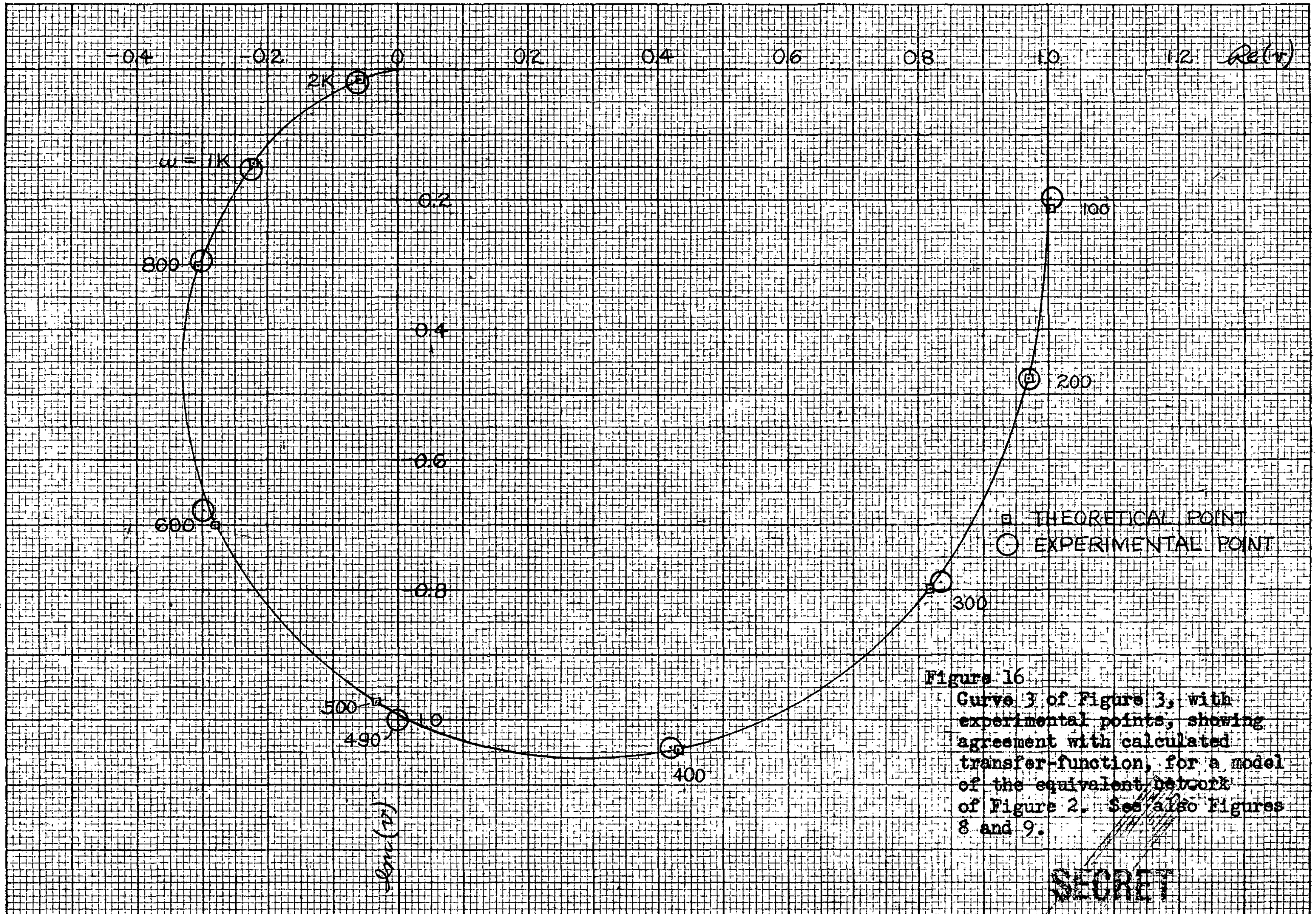

Figure 16
Curve 3 of Figure 3, with experimental points, showing agreement with calculated transfer-function, for a model of the equivalent network of Figure 2. See also Figures 8 and 9.

SECRET

186561

Appendix - <u>Derivation of Transfer-Function</u>

The transfer-functions used in the calculations were derived in the following manner:

Given the circuit of figure 2,

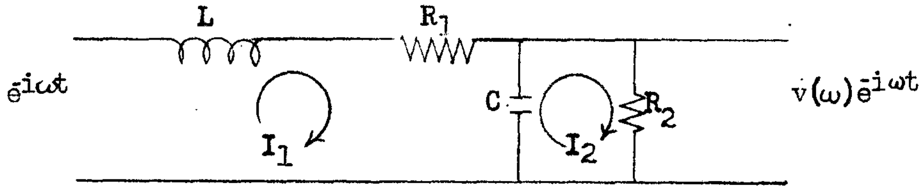

Figure 17 Circuit of figure 2 showing choice of meshes for analysis.

$X_L = \omega L$

$X_C = - \frac{1}{\omega C}$

The mesh equations are (dividing out the time-factor $e^{-i\omega t}$):

$$\left.\begin{aligned} \left[R_1 + i(X_L + X_C)\right] I_1 - iX_C I_2 &= 1 \\ -iX_C I_1 + (R_2 + iX_C) I_2 &= 0 \end{aligned}\right\} \qquad (1)$$

Solve for I_2 by use of Cramer's Rule (or by substitution) and recall that $v(\omega) = I_2 R_2$

$$v(\omega) = \frac{iX_C R_2}{\Delta} \qquad (2)$$

where

$$\Delta = \begin{vmatrix} R_1 + i(X_L + X_C) & -iX_C \\ -iX_C & R_2 + iX_C \end{vmatrix} \qquad (3)$$

expanded and simplified,

$$\Delta = (R_1 R_2 - X_L X_C) + i\left[(R_1 + R_2)X_C + R_2 X_L\right] \qquad (4)$$

To put into readily computable form, rationalize equation (2) and get

$$v(\omega) = \frac{X_C R_2}{\Delta \Delta^*} \quad \mathrm{Im}(\Delta) + i\,\mathrm{Re}(\Delta) \qquad (5)$$

where $\mathrm{Re}(\Delta)$ and $\mathrm{Im}(\Delta)$ are, as is usual, the real and imaginary parts of Δ, and Δ^* is the complex conjugate.

The function $v(\omega)$ is normalized such that for the beam on case its value at zero frequency is unity; i.e., the normalized transfer-function is

$$\tilde{v}(\omega) = \frac{v(\omega)}{v(0)} \tag{6}$$

for cases 1, 2, and 3 (beam), and

$$\tilde{v}'(\omega) = \frac{1.05}{v'(0)} \; v'(\omega) \tag{7}$$

for cases 4, 5, and 6 (no beam).

Separation of each type of operation into three cases arises from contemplated use of any of three values of filter inductor L, namely, 8, 12, and 20 millihenries, which correspond to cases 1 and 4, 2 and 5, 3 and 6, respectively.

In order to proportion the network parameters in the matter to be outlined below, and yet account for an experimental result showing (tentatively) an increase in steady-state rf voltage output of approximately 5% when the load losses are halved, the factor 1.05 is included in equation 7, making the normalized beam-off transfer-function at zero frequency $\tilde{v}'(0) = 1.05$. Further remarks on this matter are to be found below.

Calculations of Network Parameters

Designate cases thusly:

Table I

Case 1	L	$= 8 \times 10^{-3}$	Beam on
2		12×10^{-3}	Beam on
3		20×10^{-3}	Beam on
4		8×10^{-3}	Beam off
5		12×10^{-3}	Beam off
6		20×10^{-3}	Beam off

Table II

Stored energy	$U_s = 3.11 \times 10^4$ joules	(UCRL 1173)
Power-loss Beam off	$P_L' = 8.77 \times 10^6$ watts	(UCRL 1173)
Beam on	$P_L = 17.5 \times 10^6$ watts	(200-10, M4A)
Cavity frequency	$\nu_o = 12.26 \times 10^6$ sec^{-1}	(UCRL 1173)
Applied dc plate voltage	$V(0) = 2.0 \times 10^4$ volts	(EED design figure)

SUBJECT Preliminary Considerations regarding Stability of MTA Mark I as a Closed-loop System

NAME J. F. Waddell

DATE 1 November 1951

From Baker's data on operation of the Mark I oscillators at full-load and full voltage, their plate efficiency is approximately 0.75. The only data available on half-load, near-full voltage operation of the Mark I oscillators is that the rf output voltage is approximately 5% greater than for full load, full voltage operation. This for only one particular oscillator, tried only once, and there was no measurement of plate losses. The data for this one experiment, when used to find a figure for tube rf output from curves obtained from older data on these same oscillators, yields a figure for efficiency which is much lower than the experimental values for the 5831, which clustered rather closely near 0.75. Moreover, the volt-ampere figures do not agree with previous data.

In the absence of any data regarding plate losses for half-load full-voltage operation, it is necessary to estimate an efficiency factor for this type of operation. The Mark I type of oscillator, being a self-biased device, should exhibit a normal sort of behavior for a class C oscillator under conditions where the load impedance is doubled, i.e., the grid biases itself until equilibrium conditions obtain with slightly increased rf voltage output a little more than half rf current output, and tangible increase in efficiency. Rough calculations based upon the tube characteristic curves indicate a fairly good estimate for efficiency in the beam off condition to be 0.85, and for the ratio of rf output voltages to that in beam-on condition approximately 1.05.

It might be interesting to here mention the fact that the stored energy to power-loss relationships which hold for the cavity also hold for its low frequency RC equivalent circuit. Recalling the definition of Q as 2π times the ratio of energy stored at resonance to energy lost in each period of oscillation, we write

$$Q = 2\pi \frac{\nu_0 U_s}{P_L} \tag{8}$$

The time-consta-nt for decaying oscillations is

$$\tau = \frac{Q}{\pi \nu_0} \tag{9}$$

Yielding for the cavity

$$\tau = \frac{2U_s}{P_L} \tag{10}$$

For the RC shunt circuit,

$$U_s = \frac{1}{2} CV^2$$

$$P_L = \frac{V^2}{R}$$

so

$$\frac{2U_s}{P_L} = RC = \tau \tag{11}$$

the time-constant for decay of the voltage V for the circuit isolated after charging of the capacitor. Thus the equivalent circuit we are using will store the same energy per unit applied voltage at the input terminals as will the oscillator-cavity combinations, and will display the same time-constant upon decay.

From table II we calculate:

$$\left.\begin{array}{ll} \text{Beam on} & = 3.554 \times 10^{-3} \text{ sec} \\ \text{Beam off} & = 7.092 \times 10^{-3} \text{ sec} \end{array}\right\} \quad (12)$$

The driving-point impedance at zero frequency is

$$\left.\begin{array}{ll} Z(0) = R_1 + R_2 = \dfrac{V^2(0)}{P} & \text{(Beam on)} \\ Z'(0) = R_1' + R_2' = \dfrac{V^2(0)}{P'} & \text{(Beam off)} \end{array}\right\} \quad (13)$$

Since

$$\left.\begin{array}{l} P_L = 0.75\ P \\ P_L' = 0.85\ P' \end{array}\right\} \quad (14)$$

Making

$$\left.\begin{array}{l} R_1 + R_2 = 0.75\ \dfrac{V^2}{P_L} \\ R_1' + R_2' = 0.85\ \dfrac{V^2}{P_L} \end{array}\right\} \quad (15)$$

Moreover

$$\left.\begin{array}{l} \dfrac{R_2}{R_1 + R_2} = 0.75 \\ \dfrac{R_2'}{R_1' + R_2'} = 0.85 \end{array}\right\} \quad (16)$$

Thus

$$\left.\begin{array}{l} R_2 = 0.5625\ \dfrac{V^2}{P_L} \\ R_2' = 0.7225\ \dfrac{V^2}{P_L'} \end{array}\right\} \quad (17)$$

SECRET

$$\left.\begin{aligned} R_1 &= 0.1875 \frac{V^2}{P_L} \\ R_1' &= 0.1275 \frac{V^2}{P_L'} \end{aligned}\right\} \qquad (18)$$

We are now in position to calculate values for all of the parameters which are tubulated:

Table III

Case	L	R_1	R_2	C
1	8 mh	4.24 ohms	12.90 ohms	275.5 µf
2	12 mh	4.24 ohms	12.90 ohms	275.5 µf
3	20 mh	4.24 ohms	12,90 ohms	275.5 µf
		R_1'	R_2'	C'
4	8 mh	5.78 ohms	32.98 ohms	215.0 µf
5	12 mh	5.78 ohms	32.98 ohms	215.0 µf
6	20 mh	5.78 ohms	32.98 ohms	215.0 µf

From equations (4) and (5) we have

$$\mathrm{Re}\left[v(\omega)\right] = \frac{-R_2\,\mathrm{Im}\left[\Delta(\omega)\right]}{C\omega\left[\Delta\Delta^*(\omega)\right]} \qquad (19)$$

$$\mathrm{Im}\left[v(\omega)\right] = \frac{-R_2\,\mathrm{Re}\left[\Delta(\omega)\right]}{C\omega\left[\Delta\Delta^*(\omega)\right]} \qquad (20)$$

$$\mathrm{Re}\left[\Delta(\omega)\right] = R_1R_2 - X_LX_C$$

$$= R_1R_2 + \frac{L}{C} \qquad (21)$$

a constant independent of frequency.

$$\mathrm{Im}\left[\Delta(\omega)\right] = R_2L\omega - \frac{R_1 + R_2}{C\omega} \qquad (22)$$

These are the computable forms from which, using (6) and (7) the Nyquist diagrams, amplitude vs frequency, and phase vs frequency curves were calculated directly, and from which the closed-loop responses (figures 8 to 15) were calculated using equation (1) of the text.

SECRET

SECRET

DECLASSIFIED

SECRET